THE ARCHIVE OF MECHANICAL ENGINEERING

Vol. XLVII 2000 Number 4

Key words: *flight dynamics, computational fluid dynamics, grid generation, finite differences method*

TOMASZ IGLEWSKI [*)], *ZDOBYSŁAW GORAJ* [*)]

ANALYSIS OF PULL-OUT MANEUVER FOR AN AIRCRAFT REPRESENTED BY MAIN WING AND TAILPLANE, USING COUPLED EULER/FLIGHT DYNAMIC MODEL

The main aim of this analysis is to consider a mutual interference between aircraft motion and surrounding flow field. Euler flow model for inviscid, compressible gas and aircraft flight dynamics model was used to analyse quick dynamic manoeuvres. For such manoeuvres, aerodynamic hysteresis has a great influence on aircraft dynamics, which cannot be simulated with the assumption of quasi-steady aerodynamics. On the other hand, the aircraft motion as a rigid body strongly influences the flow field around itself. To account for this mutual interference, the Euler flow equations were used to obtain aerodynamic forces and moments acting on a simplified aircraft configuration (main wing + tailplane only) during pull-out manoeuvre, and the flight dynamics equations of motion were used to describe dynamics of an aircraft. Initial conditions for the flight dynamics equation of motion were settled up coming from the solution of the Euler flow model. As a test case, a weak pull-out manoeuvre was selected. During this manoeuvre, the highest value of angle of attack doesn't exceed 12 degrees - the value which can be obtained from the classical approach based on flight dynamics equations of motion with quasi-steady aerodynamics. However, coupled Euler flight dynamic model has much wider applicability, and can be used for the analysis of manoeuvres at high angles of attack, including large scale separation at sharp edges, unsteadiness and flow asymmetries even for symmetrical undisturbed flowfield case. This method, if successfully verified to a number of important flight manoeuvres (such as spin, Cobra manoeuvre, roll at high angles of attack and other) can open a new, very promising field in the analysis of aircraft dynamics.

Symbols

C_L, C_D – lift and drag coefficients,

$C_{M,WB}$ – pitching moment coefficient for wing body arrangement with respect to $^1/_4$ MAC,

[*)] *Warsaw University of Technology, Institute of Aeronautics & Applied Mechanics; ul. Nowowiejska 24,00-665 Warszawa, Poland; E-mail:goraj@meil.pw.edu.pl*

C_{LT}, C_{DT} – lift and drag coefficient for horizontal tail,
x_{ah}, z_{ah} – coordinates of horizontal tail along x and z axes in the body frame of reference,
x_{ac}, z_{ac} – coordinates of aircraft centre of gravity along x and z axes in the body frame of reference,
m – mass,
J_y – moment of inertia around y axis in the body frame of reference,
α – angle of attack,
ε – downwash in the vicinity of tailplane,
Θ – flight path angle,
ρ – air density,
V_H – flow velocity in the vicinity of tailplane,
p – local pressure,
e – internal gas energy,
T_G – temperature,
R_G – gas constant,
C_V – specific heat constant at constant volume,
δ_H – deflection of elevator,
h – flight height,
n – load factor coefficient,
U, V, W – speed components in the body frame of reference,
P, Q, R – components of the turn rate in the body frame of reference,
S_X, S_Z – static moments of inertia along X and Z axes in the body frame of reference,
F_X, F_Z – force components along X and Z axes in the body frame of reference,
M_Y – aerodynamic moment around Y axis in the body frame of reference,
N – number of iteration,
T – current time,
t_{end} – final time,
T – thrust,
$\vec{V}$ – flight speed,
$\vec{\Omega}$ – turn rate vector,
Axyz – body frame of reference (Ax - axis directed forward along the Mean Aerodynamic Chord; Az - axis in the plane of airplane symmetry perpendicular to Ax and directed downwards; Ay - axis along the right wing, perpendicular to the plane of airplane symmetry).

1. Introduction

During the last decades, we have observed an outstanding progress in aeronautical sciences [1]. Fascinating achievements of Computational Fluid

Dynamics, super- and hiper- manoeuvrability, modern avionics and technology of new materials have created the newest generation of combat, agile aircraft. F-22, Rafale, Typhoon, JAS 39-Grippen, F/A-18 E/F, Su-37 are good examples. Ability to fly at the post-stall angles of attack with great angular velocities opens the door for discovery of brand new air combat manoeuvres. Most of these manoeuvres are very dangerous because of stall/spin hazard, plane structure limits or crew physical limits. Every new idea should first be investigated before performing full scale flight tests. For the most cases, it is not possible to simulate the high alpha manoeuvres using wind tunnels. The only way of investigation is to perform a numerical simulation. In typical approach one uses an aircraft flight dynamic model, assuming quasi-steady aerodynamic characteristics. However, at high-alpha quick dynamic manoeuvres, this assumption does not hold true. The flow around an aircraft can be largely separated, unsteady, containing vortices etc. Aerodynamic hysteresis may appear.

But over the past half century, we have witnessed the rise to importance of a new methodology for solving the complex problems in fluid mechanics. This new methodology has become known as Computational Fluid Dynamics. In this computational approach, the equations that govern the process of interest are solved numerically. Today CFD can routinely handle many types of flowfields [2]. One can obtain pressure distribution on aircraft surfaces, separation regions, downwash, local air velocities etc., everything what is needed to complete flight model for the dynamic high-alpha manoeuvres.

The progress in CFD is closely tied to the development of a high speed digital computers. Today there are many types of different CFD codes, flow models, types of discretization etc. To perform a simulation, one has to choose the model, generate a computational grid and choose the scheme to solve the governing equations [3]. The most important thing is to use the proper model for the proper flow type, for example Navier-Stokes equations with model of turbulence for viscid, compressible, turbulent flow; Euler equations for compressible inviscid fluid or Laplace equation for simple potential flows. One must consider the advantages and disadvantages of each approach. Using Navier-Stokes equations one can obtain shear layer details, turbulence, viscid separation regions etc. But computational cost is much higher than, for example, for Euler model which can be sufficient for many cases.

There are at least three main methods of discretization of governing equations: finite volumes, finite elements and finite differences [4]. The simplest, frequently used and succesfull approach to the discretization problem is to use the governing equations in conservative form and apply the finite difference scheme. It means that the governing equations have a discrete representation on computational grid, and every derivative in computational area is represented by a finite difference value, obtained using data from neighbouring grid points. Such an approach was used in this paper.

To solve the governing equations efficiently, a proper numerical method has

to be selected. One can choose from a great number of explicit and implicit methods. An explicit scheme is the one for which only one unknown appears in the difference equation in such a way that it permits to compute this unknown in terms of the known quantities (Lax-Wendroff, MacCormack, Euler Explicid etc.), [5]. An implicit method requires that discretized difference equation must be written at all interior grid points, resulting in a system of algebraic equations from which all unknowns for all grid points have to be solved simultaneously (for example Euler Implicit, Laasonen, Trapezoidal Differencing etc.). In this paper the MacCormack two stage explicit method [5] was used.

The main difference between classical CFD and coupled CFD/flight dynamics approach to flow analysis consists in dealing with curved flight paths or rotating bodies. In classical CFD, the flow is investigated using movable frame of reference, fixed to the airplane, usually at constant angle of attack and sideslip. In the coupled CFD/flight dynamics approach – developed in this paper – the flow is investigated also at movable frame of reference. However, in this instance the flow phenomena involved by path curvature were modelled due to changeable angles of attack and sideslip, and other phenomena involved by airplane rotations were simulated by means of "virtual" rotations of the whole flowfield with respect to the airplane. Results obtained from the coupled CFD / flight dynamics approach were compared to the classical, pure flight dynamics approach.

2. Physical model

Constant air density for the flight dynamics model was assumed. For flow field model the following boundary conditions were assumed: air density and pressure correspond to those of starting flight level, air velocity and angle of attack correspond to those of aircraft flight velocity and aircraft angle of attack in the flight dynamics model. Symmetrical flight [6], [7] and symmetrical flow field were considered only. For a direct flow field simulation there is a need to generate grid in the wide field around the whole body. It would be very difficult to surround the whole aircraft body with a grid being regular enough. The real aircraft was simplified and represented by the wing + horizontal tail configuration. It was assumed that perturbations in flow can propagate downstream only, so any influence of the horizontal tailplane on the main wing flow was neglected. Velocity loss, downwash [8] and air density in the tailplane vicinity were determined from the flow equations. These parameters were used to calculate aerodynamic forces acting on horizontal tailplane for flight dynamic model.

Numerical example was performed for I-22 airplane, so wing and tailplane geometry, their mutual position, mass, moments of inertia and propulsion characteristics were taken just for this airplane. NACA-0010 wing section [9] was assumed for the main wing geometry. As a test case, the pull-out manoeuvre was considered (Fig. 9).

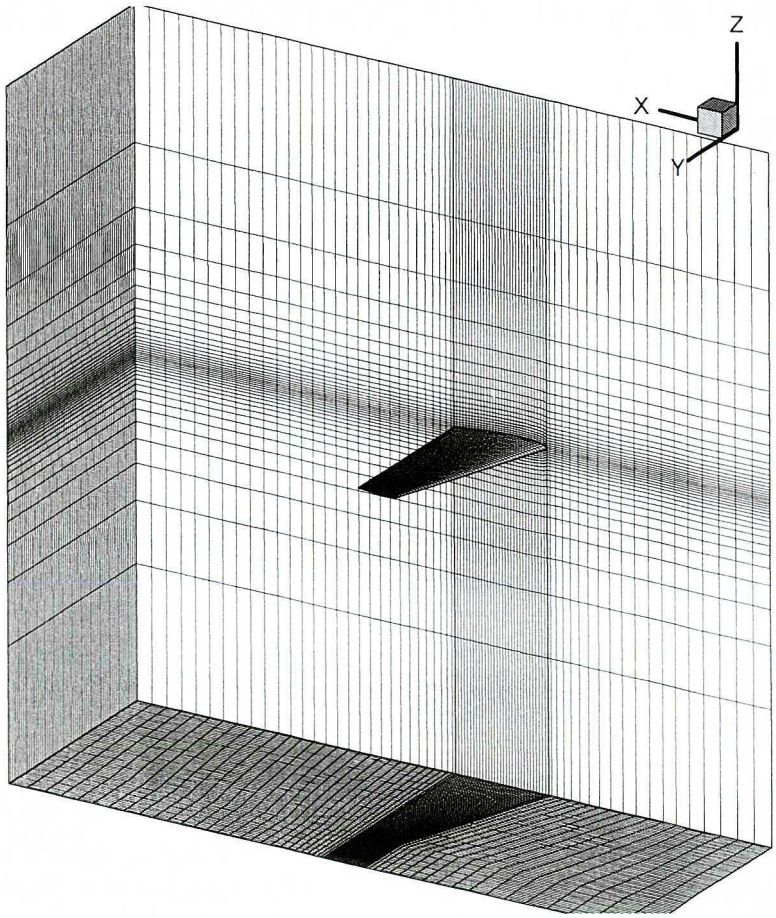

Fig. 1. Grid for Euler model

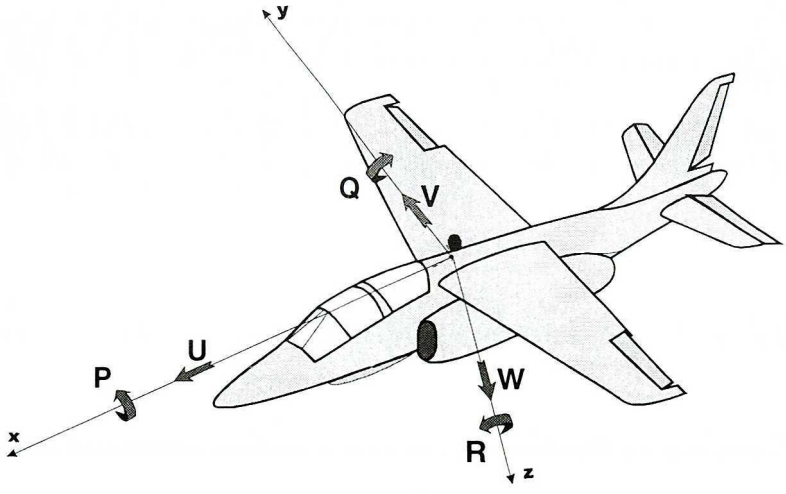

Fig. 2. Linear and angular velocity components in the body frame of system

3. Mathematical models

a) flight dynamics model

Flight dynamic equations of symmetrical motion [6] were used in the following form:

$$\begin{aligned} m\left(\dot{U}+Q\cdot W\right)-S_x\cdot Q^2+S_z\cdot\dot{Q}&=F_X,\\ m\left(\dot{W}-Q\cdot U\right)-S_x\cdot\dot{Q}-S_z\cdot Q^2&=F_Z,\\ J_y\cdot\dot{Q}-S_x\left(\dot{W}-U\cdot Q\right)+S_z\left(\dot{U}+Q\cdot W\right)&=M_Y,\\ \dot{\theta}&=Q. \end{aligned} \tag{1}$$

Forces F_X, F_Z and moment M_Y represent full aerodynamic loads, so there is no need to consider aerodynamic derivatives usually used in classical approach to flight dynamic simulation.

b) flow field model

Compressible and inviscid flow of perfect gas was assumed. Euler equations in conservative form [4], [10], [11] were used in the following form:

- continuity equation

$$\frac{\partial\rho}{\partial t}+\nabla\cdot\left(\rho\cdot\vec{V}\right)=0, \tag{2}$$

- three momentum equations:

$$\frac{\partial\left(\rho\cdot U\right)}{\partial t}+\nabla\cdot\left(\rho U\cdot\vec{V}\right)+\frac{\partial p}{\partial x}=0, \tag{3}$$

$$\frac{\partial\left(\rho\cdot V\right)}{\partial t}+\nabla\cdot\left(\rho V\cdot\vec{V}\right)+\frac{\partial p}{\partial y}=0, \tag{4}$$

$$\frac{\partial\left(\rho W\right)}{\partial t}+\nabla\cdot\left(\rho W\cdot\vec{V}\right)+\frac{\partial p}{\partial z}=0, \tag{5}$$

- energy equation

$$\frac{\partial}{\partial t}\left[\rho\left(e+\frac{\left|\vec{V}\right|^2}{2}\right)\right]+\nabla\cdot\left[\rho\left(e+\frac{\left|\vec{V}\right|^2}{2}\right)\vec{V}\right]+\frac{\partial\left(U\cdot p\right)}{\partial x}+\frac{\partial\left(V\cdot p\right)}{\partial y}+\frac{\partial\left(W\cdot p\right)}{\partial z}=0. \tag{6}$$

In the above equations, there are the following unknowns: air density ρ; three velocity components U,V,W; internal gas energy e and pressure p. To close this system, the following two relationships were used:

- equation of state for perfect gas

$$p = \rho \cdot R_G \cdot T_G , \tag{7}$$

and

- thermodynamic relationship between energy and temperature

$$e = c_v \cdot T_G = \frac{p}{\rho \cdot (\gamma - 1)} . \tag{8}$$

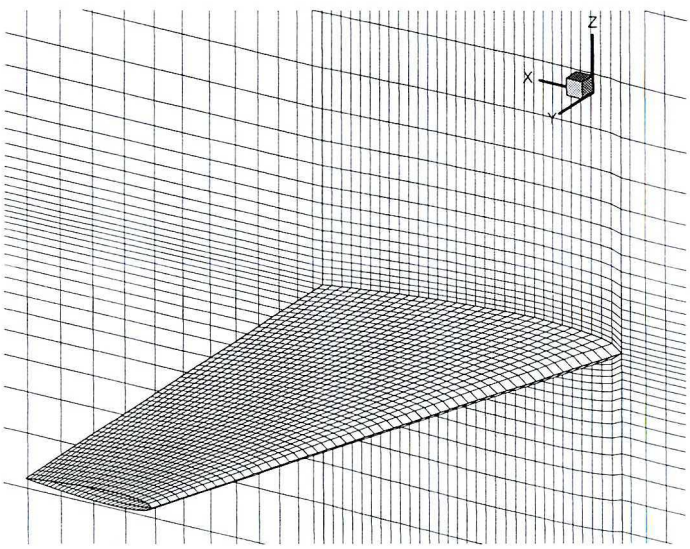

Fig. 3. Grid on the wing surface

MacCormack finite differences scheme [3] was used as a numerical method for solving the Euler flow equations. Far field boundary conditions [12] were determined coming from the flight dynamics model. Airplane velocity components in the body frame of system were computed having known the angle of attack of an airplane and its speed. Air density and pressure correspond to the flight height. From boundary condition on the wing surface it follows that the local flow vector is tangent to the local surface [5]. 225200 grid points in five connected structural grid blocks were used in computations.

4. Flow and flight simulation

Initial conditions were determined coming from steady, level flight conditions. Aerodynamic characteristics of wing + tailplane configuration versus angle of attack for different speeds were computed from equations (2÷8). Next, these characteristics were used to determine initial parameters (α, δ_H, T) at a steady level flight. This process is graphically presented in Fig. 4.

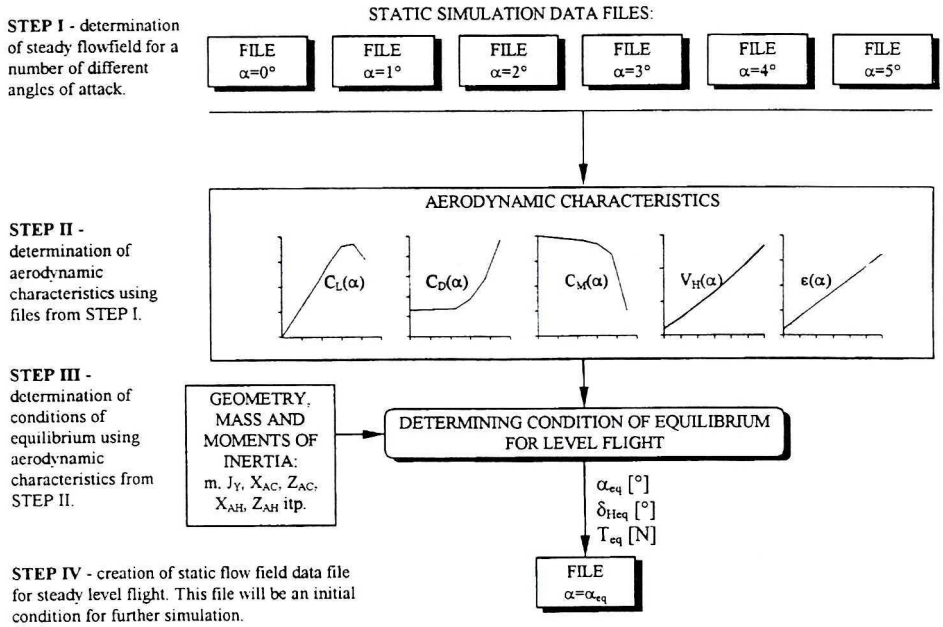

Fig. 4. Determination of initial conditions (symbol „eq" corresponds to conditions of equilibrium)

Fig. 5 shows a scheme of coupling of the flow model and flight dynamic model. Fig. 6 presents the data transfer scheme during simulation. Files are permanently saved in each 0.1 second time during the simulation process. These files contain local flow field data: pressure, velocity density and other parameters.

The main difference between classical CFD and coupled CFD/flight dynamics approach to flow analysis consists in dealing with curved flight paths or rotating bodies. In classical CFD the flow is investigated using movable frame of reference, fixed to the airplane, usually at constant angle of attack and sideslip. In coupled CFD/flight dynamics approach, the flow is investigated also at movable frame of reference. However, for this case the flow phenomena corresponding to path curvature can be modelled due to changeable angles of attack and sideslip, and the phenomena corresponding to airplane rotations can be simulated due to relative rotations of the whole flowfield with respect to the airplane. Airplane rotations around its centre of gravity modify the whole flowfield in its vicinity. Flow field modification was accounted for into analysis adding an increment of velocity to each velocity component at each grid point (Fig. 7). This increment is a difference between the linear velocity component at current and former time step.

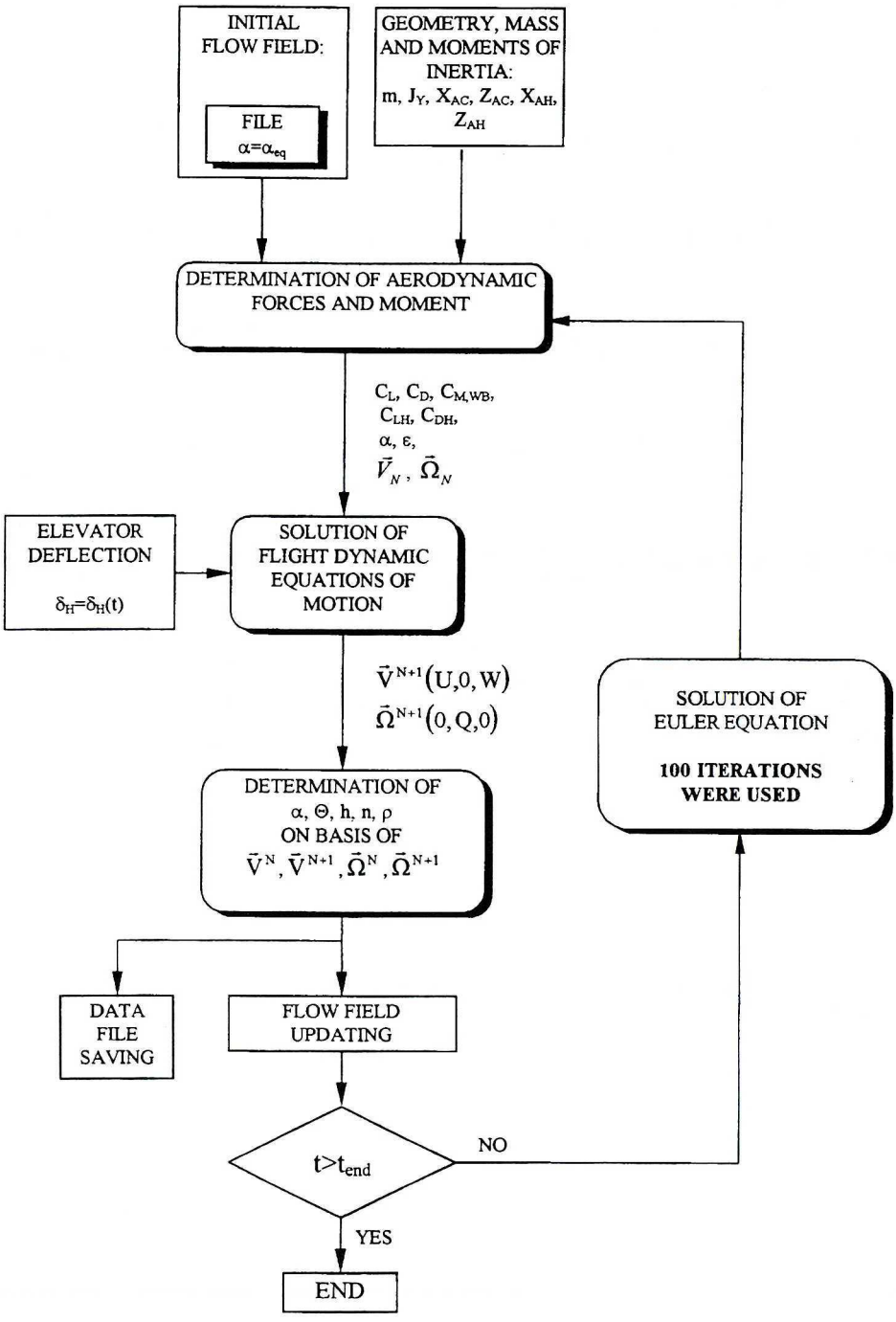

Fig. 5. Chart flow simulation using two coupled models

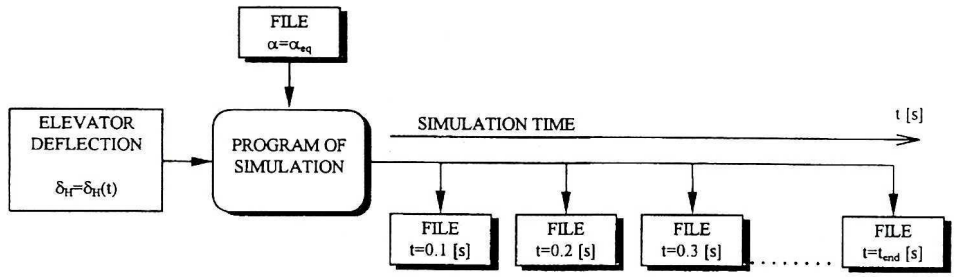

Fig. 6. Data transfer scheme

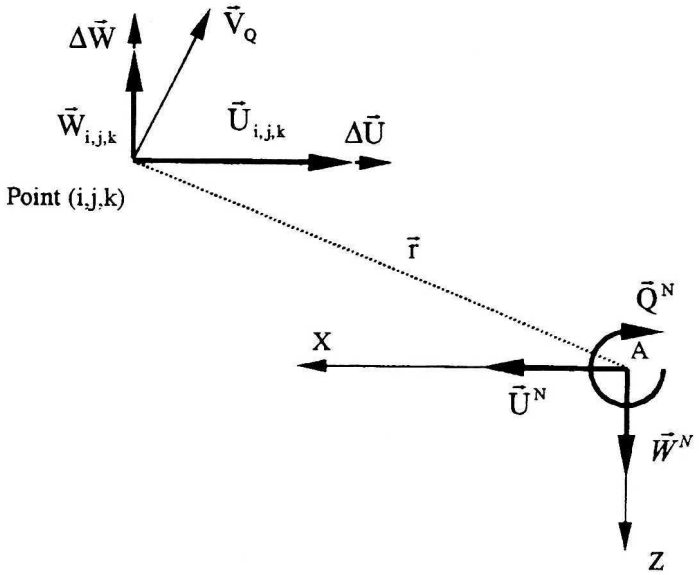

$$\begin{aligned} \Delta U &= U^N - U^{N-1}, \\ \Delta W &= W^N - W^{N-1}, \\ \vec{V}_Q &= \vec{Q}\times\vec{r}\,. \end{aligned} \tag{9}$$

Fig. 7. Flow field modification scheme for a point (i,j,k)

Each velocity component at every grid point was updated immediately after the solution of flight dynamics equations of motion was obtained, according to the following relations:

$$U^N_{i,j,k} = U^{N-1}_{i,j,k} + \left(U^N - U^{N-1}\right) + \left(V^N_{QX} - V^{N-1}_{QX}\right), \tag{10}$$

$$V^N_{i,j,k} = V^{N-1}_{i,j,k} \text{ - because of the symmetrical flight assumption,} \tag{11}$$

$$W^{N}_{i,j,k} = W^{N-1}_{i,j,k} + \left(W^{N} - W^{N-1}\right) + \left(V^{N}_{QZ} - V^{N-1}_{QZ}\right). \tag{12}$$

Flow field modification can be treated as a transient process after a temporary disorder involved by a strong impulse (Fig. 8). Each time step in the solution of flight dynamics equations of motion and the flow field modification are well visible as a top value after each 100 iterations. Number 100 was selected arbrary (from Fig.8 it is visible that 30 or 40 is sufficient to suppress the velocity derivative and only 10 or 20 to suppress the density derivative). Euler equations (2÷6) are written and then solved in dimensional form. Because initial undisturbed flow velocity is much greater than 100 m/s, and undisturbed density is closed to unity, so the velocity residuum of order unity and the density residuum of order one percent seems to be acceptable. Therefore, if residua go under an assumed acceptable level at all field points, the process of solving for a prescribed time point is stopped and a transition to the next time point is performed. It should be emphasised that in the case of more rapid manoeuvres the number of necessary iterations can increase over 100. However, a specific number of iterations must be chosen coming from a graph like that of in Fig.8.

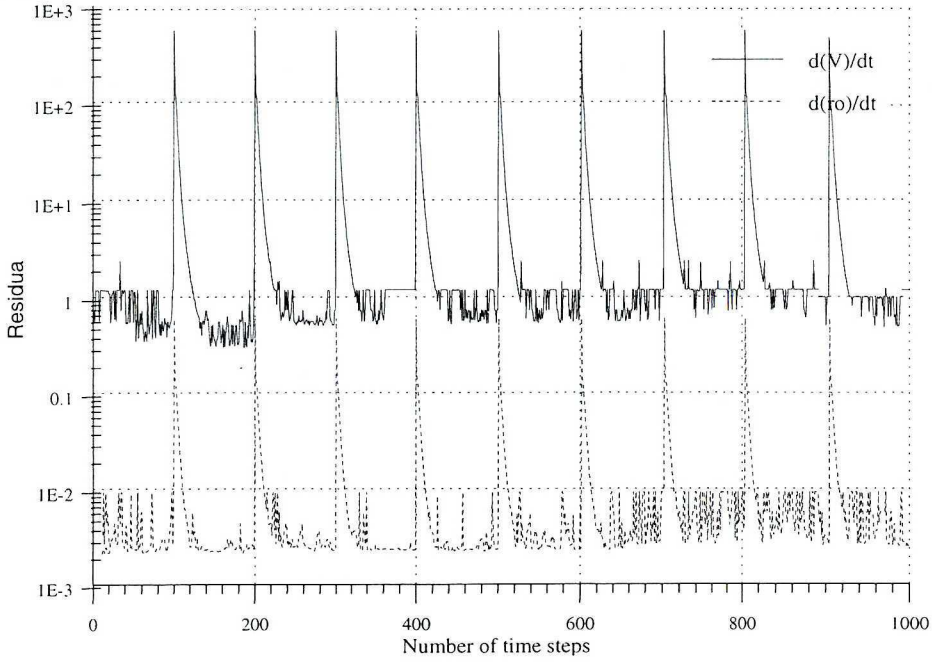

Fig. 8. Residua of $\frac{dV}{dt}$ and $\frac{d\rho}{dt}$ versus time

4. Results of simulation

As a test case, a pull-out manoeuvre was selected. Airplane was initially in a steady, level flight. Pull-out was initiated by deflection of elevator, according to the function shown in Fig. 9. Selected airplane responses are presented in Fig. 10÷16. In Fig. 10÷13 results obtained from the coupled Euler/flight dynamics model were compared to that of classical pure flight dynamics model.

Fig. 10 shows flight paths in the plane of airplane symmetry. Aircraft begins climbing due to negative elevator deflection. One can see that maximum altitude difference between coupled models and pure flight dynamics model does not exceed 10 meters. Final difference between both models at a distance of 1500 meters is about 1.9 meter. Angle of attack versus time is presented in Fig. 11. Aircraft rapidly increases angle of attack when elevator is deflected (see Fig. 9). In Fig. 11 one can see short period oscillations as a result of disturbing of the airplane out of steady flight. These oscillations have a positive damping coefficient and a period of about 0.9 s. Amplitude, damping coefficient and period are similar for both coupled and pure flight dynamics model. It is significant that damping of oscillations in coupled Euler - flight dynamics model is achieved due to direct influence of flow to aircraft body. In classical approach, damping of oscillations is realised due to the so-called stability derivatives.

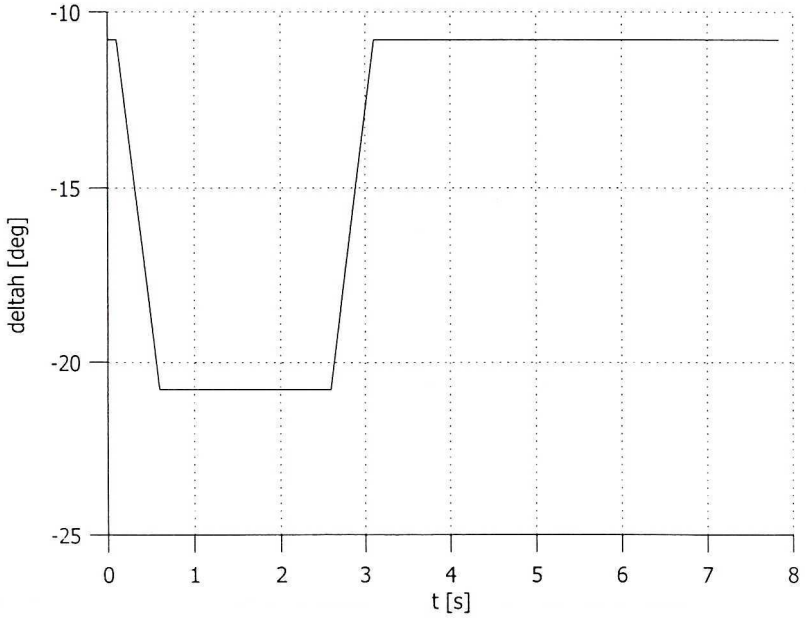

Fig. 9. Elevator deflection versus time

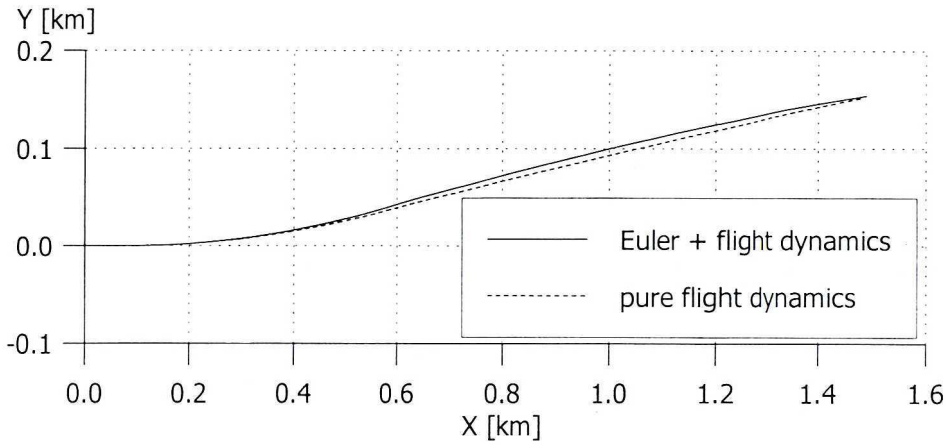

Fig. 10. Flight path comparison

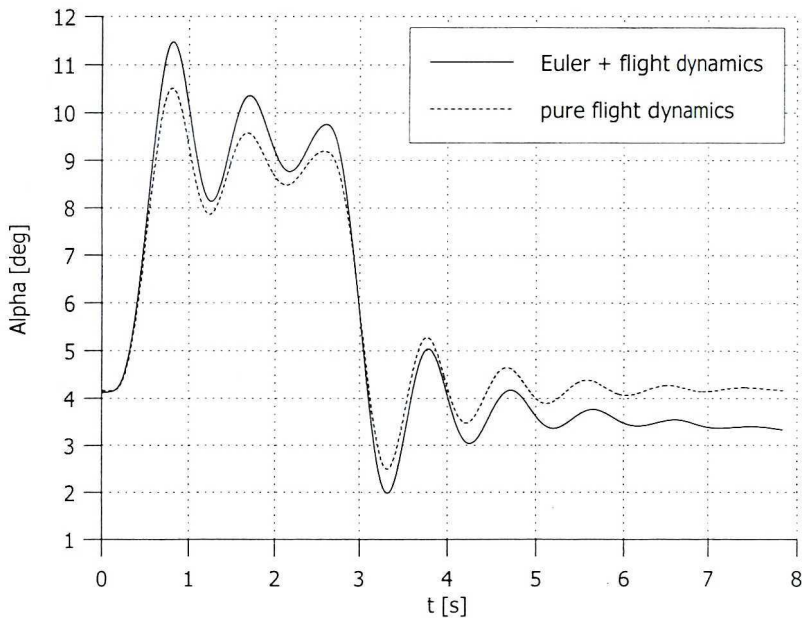

Fig. 11. Angle of attack versus time for two different models: Euler + flight dynamics and pure flight dynamics

Fig. 12 presents comparison between the velocity losses in the pull-out manoeuvre determined from the two models. It can be seen that velocity loss ratio is much higher in first three seconds of manoeuvre - when aircraft is at high angles of attack - because of higher drag. Maximum difference between both models is equal approximately to 1 m/s after 8 seconds of flight. Load factor coefficient versus time is presented in Fig. 13. Values are similar for coupled and classical models. Differences in coefficient values after the fourth second of flight are a result of different flight path curvature (see Fig. 10). Fig. 14÷16 present lift coefficients versus angle of attack. One can see an influence of aerodynamic hysteresis. There is a difference in lift coefficients during increasing and decreasing phase of angle of attack. In classical approach, this phenomenon (i.e. hysteresis) cannot be taken into consideration.

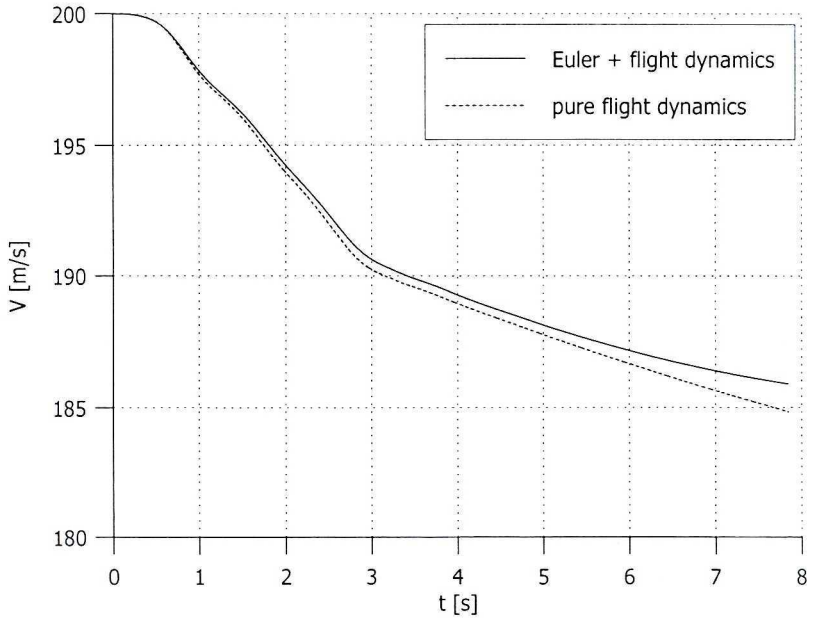

Fig. 12. Flight speed versus time for two different models: Euler + flight dynamics and pure flight dynamics

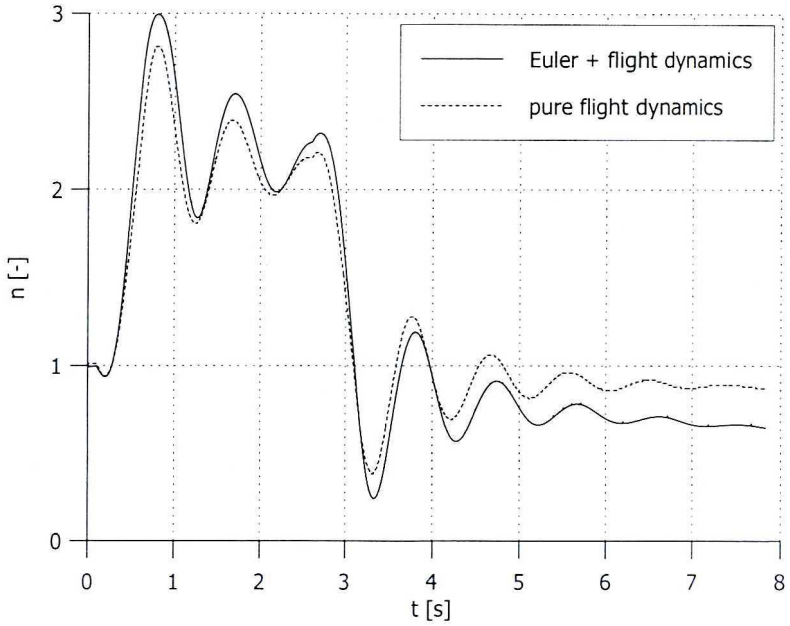

Fig. 13. Load factor coefficients versus time for two different models: Euler + flight dynamics and pure flight dynamics

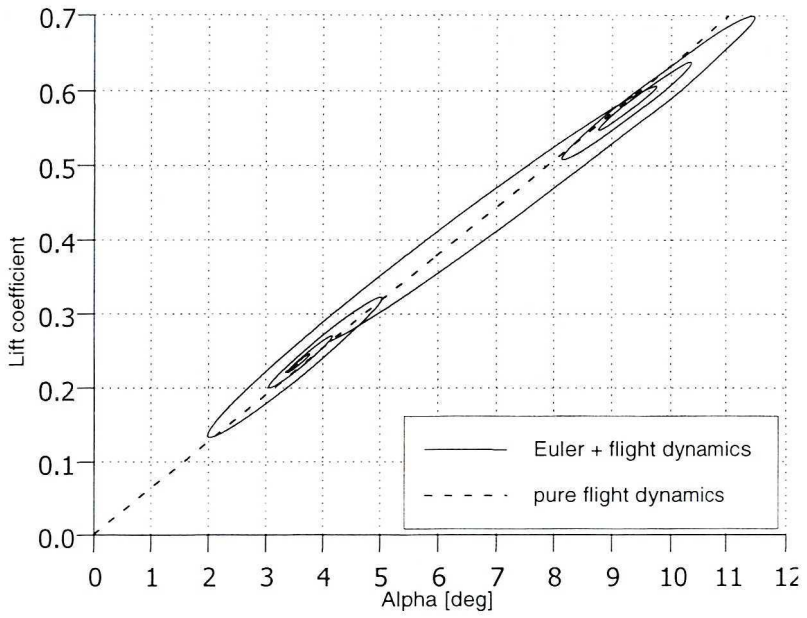

Fig. 14. Lift coefficient (visible hysteresis) for two different models: Euler + flight dynamics and pure flight dynamics

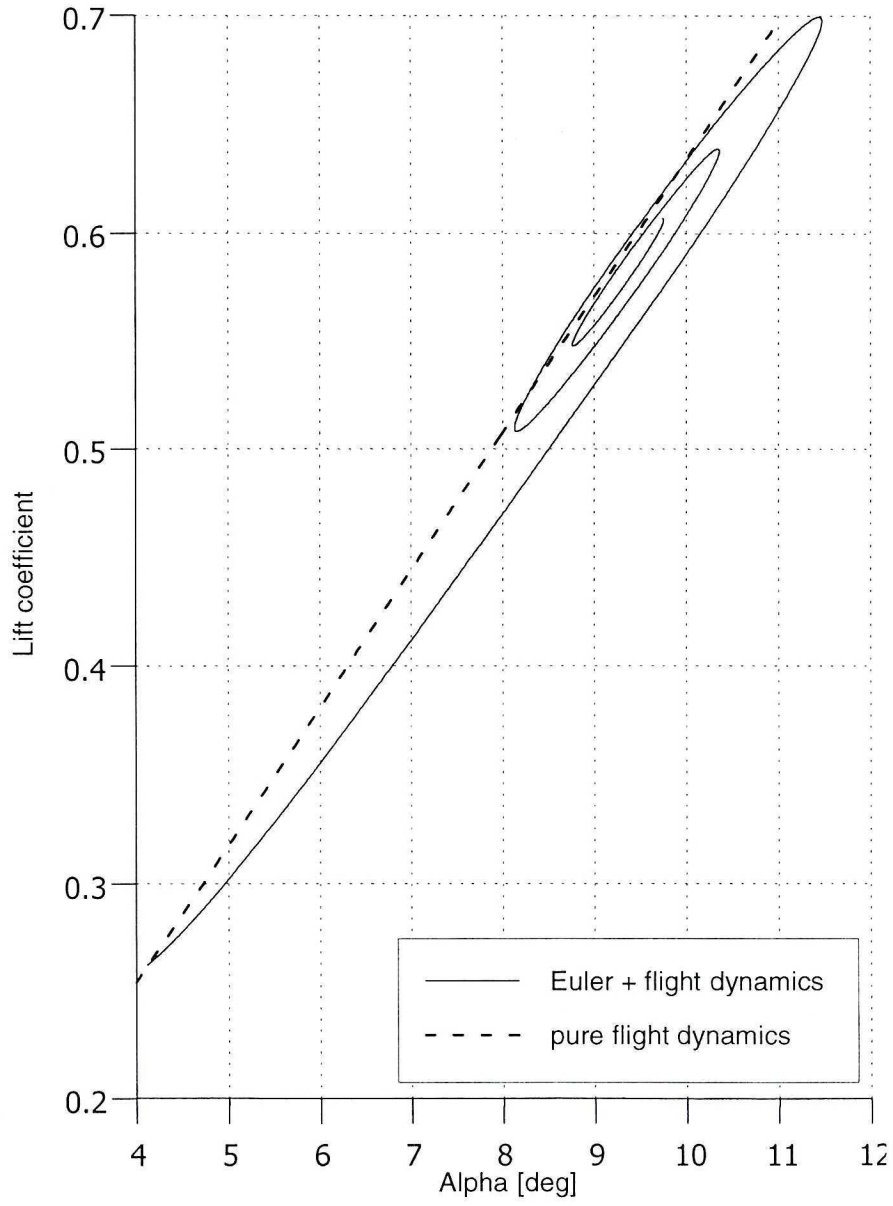

Fig. 15. Lift coefficient versus angle of attack during entry at high AoA for two different models: Euler + flight dynamics and pure flight dynamics

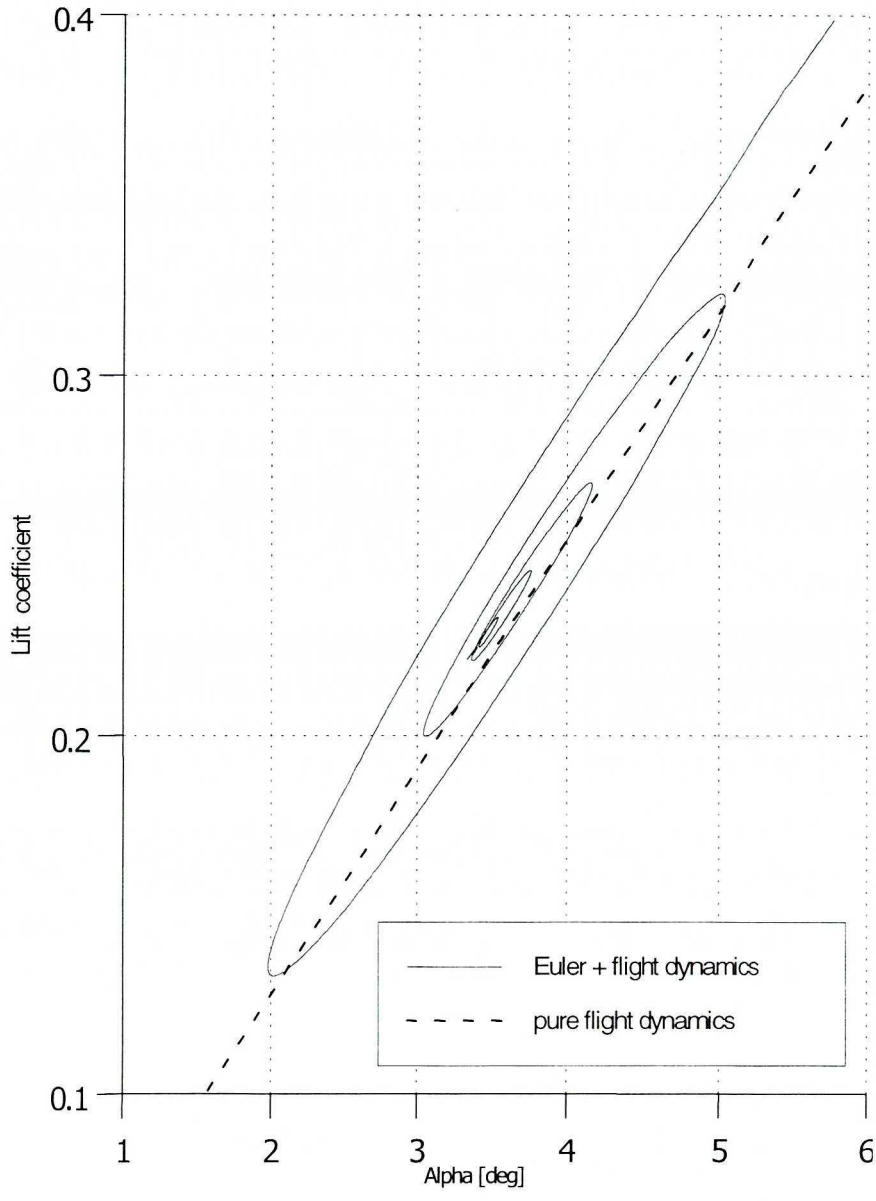

Fig. 16. Lift coefficient versus angle of attack during return to low AoA for two different models: Euler + flight dynamics and pure flight dynamics

6. Conclusion

Extensive progress in CFD and appearance of high-speed/low-cost computers made it possible to couple Euler flow model and flight dynamics model. Using CFD codes instead of quasi-steady aerodynamics gives an opportunity to reveal a wide range of aerodynamic effects: aerodynamic hysteresis, unsteadiness, vortex flow, shock waves etc. The test case considered here — a pull-out manoeuvre — cannot demonstrate the high-alpha effects, because the angle of attack doesn't exceed twelve degrees. For this range of angles of attack, there is a little difference between coupled Euler — flight dynamics and the pure flight dynamics models. Using coupled Euler — flight dynamics model enables us to reveal aerodynamic hysteresis what confirms the utility of the presented method to simulate rapid dynamic manoeuvres. For such a low range of angles of attack, one can see a sufficient convergence between results of the presented and the classical approach despite significant differences between both models. Additionally, the programme generates a great number of flow data. One can get pressure and velocity fields, data describing separations, position and shape of shock waves etc. as a function of manoeuvre time. This can be very useful in the analysis and design of combat aircraft. A simplified configuration was investigated here, however, it is possible to analyse the whole aircraft using more dense and refined grid. Unfortunately, this method demands a high speed and large memory computers. However, analysing the trends in computer progress one can predict that in the nearest future long time of calculation will not a problem. Another weak point of the presented method is a difficulty in grid generation for more intricate shapes. In some cases, the use of unstructured grids can save time of pre-processing.

Manuscript received by Editorial Board, June 28, 2000;
final version, November 03, 2000.

REFERENCES

[1] Goraj Z.: New Directions of Research in Aeronautical Engineering - Breaking the Barriers. Journal of Theoretical and Applied Mechanics, 4, 35,1997, pp.781÷812.

[2] Strohmeyer D., Orlowski M., Longo J.M.A., Hummel D., Bergmann A.: An Analysis of Vortex Breakdown Predicted by the Euler Equations. ICAS Paper 96-1.6.3.

[3] Tannehill J.C., Anderson D.A., Pletcher R.H.: Computational Fluid Mechanics andHeat Transfer. Taylor&Francis, Washington 1997.

[4] Hirsch C.: Numerical Computation of Internal and External Flows. Vol 1-2, 1988.

[5] Anderson J. D.: Computational Fluid Dynamics, McGraw-Hill, New York 1995.

[6] Goraj Z.: Calculations of Equilibrium. Maneuverability and Stability of an Aircraft in Subsonic Range of Speed (in polish), Warsaw University of Technology, Warsaw 1984.

[7] Cook M.V.: Flight Dynamics Principles, Arnold, London 1997.

[8] Stinton D.: The Design of the Aeroplane. BSP Professional Books, London 1989.

[9] Abbott I., Doenhoff A.: Theory of Wing Sections. Dover Publications,New York 1959.

[10] Wendt J. (Ed.): Computational Fluid Dynamics. Springer Series, 1996.

[11] Fletcher C.A.J.: Computational Techniques for Fluid Dynamics. Vol.1-2, Springer Series, 1987.

[12] Peyret Roger (Ed.): Handbook of Computational Fluid Mechanics. Academic Press Ltd., London 1996.

Analiza manewru wyrwania dla modelu samolotu reprezentowanego płatem głównym i usterzeniem poziomym przy użyciu połączonych modeli dynamiki (równania ruchu samolotu) i opływu (model Eulera)

Streszczenie

Celem pracy jest zbadanie wzajemnych sprzężeń pomiędzy ruchem samolotu a polem przepływu. Zaprezentowano w niej możliwość powiązania dynamicznych równań ruchu samolotu z równaniami Eulera opisującymi ruch nielepkiego, ściśliwego gazu w celu symulacji szybkich, dynamicznych manewrów samolotu. Dla tego typu manewrów histereza aerodynamiczna ma duży wpływ na ruch samolotu i założenie quasi-ustalonych charakterystyk aerodynamicznych może prowadzić do błędów w wynikach symulacji. Równania Eulera wykorzystane zostały do określenia sił i momentów aerodynamicznych działających na uproszczony model samolotu, reprezentowany przez płat główny i usterzenie wysokości. Dane te zostały następnie użyte w dynamicznych równaniach ruchu samolotu zamiast quasi-ustalonych charakterystyk aerodynamicznych. Wyniki porównano z wynikami podejścia klasycznego - uzyskanymi z dynamicznych równań ruchu przy założeniu quasi-ustalonej aerodynamiki.